Models with all the right curves

Nahidul Khan

Jonathan Smith

Michael Hinchey

Khan, Smith and Hinchey show that computational fluid dynamics can be used to predict the behaviour of water current turbines.

Who should read this paper?

Anyone with an interest in generating renewable energy from ocean currents, and particularly those who may be looking for an economical means to power autonomous subsea instruments.

Why is it important?

In the marine world, as in other remote and harsh environments, simulation offers definite advantages for development and testing of new technologies. A well-worn tool for simulating the complex interactions between fluids and real-world objects, such as ocean currents and turbines, is 'computational fluid dynamics' (CFD). From previous work published in the JOT, the authors have determined that Savonius rotors may be used in turbines for micro-power applications in low speed currents, and that it is possible to accurately estimate the amount of power that could be generated by a Savonius rotor of a given size in an ocean current of a given speed. In this paper, the authors take their investigation to the next step by proving it is possible to use CFD to predict the behaviour of a Savonius rotor under differing current conditions. Full scale turbines are expensive to build and difficult to deploy. The results of this work confirm that CFD can be used to tune the turbine design before it is built.

The authors submit that small scale versions of the Savonius rotor could be used now to generate micro-power from ocean currents or in rivers. Larger, high capacity devices will take longer to come into commercial use.

About the authors

Nahidul Khan received a BEng (2007) in Electrical Engineering from Bangladesh University of Engineering and Technology; a M.Eng. (2008) from Memorial University of Newfoundland (MUN); and is currently working towards a PhD in the Faculty of Engineering and Applied Science at MUN. His research interests centre around water current energy. Jonathan Smith holds a BEng (2011) in Mechanical Engineering from MUN and is presently doing a MEng at MUN part time on the development of a miniature autonomous underwater vehicle. Michael Hinchey is a Professor of Mechanical Engineering at MUN. He holds a PhD (1979) from the University of Toronto Institute for Aerospace Studies. His main areas of expertise are fluids and controls.

[Editor's note: This is the third in a series of papers published by the authors on this topic. Earlier papers may be found in Volume 4, Number 2 and Volume 5, Number 2.]

A CFD STUDY OF A SAVONIUS WATER CURRENT TURBINE

Nahidul Khan[1], Jonathan Smith[2], Michael Hinchey[3]
[1]Nalcor Energy, Bay D'Espoir, NL, Canada
[2]Schlumberger, Calgary, AB, Canada
[3]Memorial University of Newfoundland, St. John's, NL, Canada

ABSTRACT

In earlier work, we tested the Savonius rotor as a water current turbine. Here we explore the possibility of studying the behaviour of the rotor using the Computational Fluid Dynamics (CFD) software package FLOW 3D. The paper shows that CFD can predict the basic behaviour of the rotor as seen in the experiment. This result is important because running CFD takes much less time and is much less expensive than running experiments. So we can now use CFD to optimize the geometry and explore strategies for control.

KEY WORDS

Savonius rotor; Tip speed ratio; Power coefficient; Computational Fluid Dynamics

NOMENCLATURE

A	=	profile area
A B C	=	source terms
C	=	constants
c	=	sound speed
C_P	=	power coefficient
C_S	=	speed coefficient
G	=	generation function
k	=	turbulence intensity
ε	=	turbulence dissipation
M	=	PDE unknown
N	=	PDE rate
P	=	dynamic pressure
$\mathbf{P}$	=	power
Q	=	volumetric flow rate
R	=	tip radius
S	=	stream speed
t	=	time
T	=	production function
D	=	dissipation function
U V W	=	water velocities
x y z	=	Cartesian grid
α β	=	constants
ρ	=	water density
ω	=	rotational speed
λ	=	tip speed ratio
μ	=	water effective viscosity
μ_l	=	water laminar viscosity
μ_t	=	water eddy viscosity

INTRODUCTION

This work is part of a much larger project known as the Seaformatics project. The goal of that project is to develop an array of instrumentation pods that can be deployed on the seabed for exploration of resources beneath it. The pods are to be powered by the local current. In earlier work [Khan et al., 2009], we explored use of the Savonius rotor, which was developed initially as a wind turbine, for this application. The work obtained data for the rotor from a series of model tests. Here we explore the possibility of studying the rotor behaviour using the Computational Fluid Dynamics (CFD) software package FLOW 3D [Flow Science, n.d.].

SCALING LAWS OF TURBINES

For turbomachines, we are interested mainly in the power of the device as a function of its rotational speed. We generally present data in a nondimensional format so it can predict prototype behaviour. The simplest way to develop a nondimensional power is to divide power $\mathbf{P}$ by something which has the units of power. The power in a flow is its dynamic pressure P times volumetric flow rate Q.

The dynamic pressure is

$$P = \rho S^2/2$$

where ρ denotes the density of fluid and S is the speed of the flow. Flow rate Q is the speed of the flow S times the profile area of the turbine A:

$$Q = S\ A$$

So, a reference power is

$$P\ Q = [\ \rho S^2/2\ ]\ SA$$

So, we can define a power coefficient C_P

$$C_P = \mathbf{P}\ /\ [\ A\ \rho S^3/2\ ]$$

To develop a nondimensional version of the rotational speed of the turbine, we can divide the tip speed of the blades or buckets Rω by the flow speed S. So, we can define a speed coefficient C_S

$$C_S = [\ R\omega\ ]\ /\ S$$

These coefficients can be found in most papers on turbines. It is customary to use the symbol λ instead of C_S and call it the tip speed ratio.

SAVONIUS WATER CURRENT TURBINE

On the positive side, the Savonius water current turbine is simple and easy to build. It is robust, and it has low maintenance. It accepts flow from all directions, and it has high starting torque. On the negative side, it has low efficiency and a slow running speed. The basic rotor [Savonius, 1931] consists of two semicircular buckets with a small overlap between them. Figure 1 shows the rotor tested in earlier work. Three different sizes of the rotor were tested.

EXPERIMENTAL RESULTS

Experiments were carried out in the wave tank at Memorial University of Newfoundland. The wave tank is 54 m x 5 m x 3 m. It is equipped with a towing carriage with a maximum speed of 5 m/s. The motion of the carriage was used in this work to simulate a current. The rotor was held in a box that had almost fully open vertical sides but had fully closed top and

Figure 1: The experimental Savonius rotor.

bottom plates. Torque was measured by a brake dynamometer. A brake arm, attached to the rotor shaft, pushed against a load cell. Rotational speed was measured using an encoder. Figure 2 shows the experimental power output of the rotor [Khan et al., 2010]. Each green swath of data is for a particular brake setting, and it shows that the power and the speed varied during each rotation cycle. The black circles in the swaths are cycle averages.

COMPUTATIONAL FLUID DYNAMICS

There are only a few Computational Fluid Dynamics (CFD) software packages that are able to model flow around the Savonius rotor. Here we use FLOW 3D. In FLOW 3D, the flow field is discretized by a fixed Cartesian or xyz system of grid lines. Small volumes or cells surround points where grid lines cross. Hydrodynamics flows are generally turbulent. Engineers are usually not interested in the details of the eddy motion in a turbulent flow. Instead they need models which account for their diffusive character. These can be obtained from the momentum equations through a complex time averaging process. These models are known as eddy viscosity models.

Conservation of momentum considerations give:

$$\rho\,(\,\partial U/\partial t + U\partial U/\partial x + V\partial U/\partial y + W\partial U/\partial z\,) + A = -\,\partial P/\partial x + [\,\partial/\partial x\,(\mu\partial U/\partial x) + \partial/\partial y\,(\mu\partial U/\partial y) + \partial/\partial z\,(\mu\partial U/\partial z)\,]$$

$$\rho\,(\,\partial V/\partial t + U\partial V/\partial x + V\partial V/\partial y + W\partial V/\partial z\,) + B = -\,\partial P/\partial y + [\,\partial/\partial x\,(\mu\partial V/\partial x) + \partial/\partial y\,(\mu\partial V/\partial y) + \partial/\partial z\,(\mu\partial V/\partial z)\,]$$

$$\rho\,(\,\partial W/\partial t + U\partial W/\partial x + V\partial W/\partial y + W\partial W/\partial z\,) + C = -\,\partial P/\partial z - \rho g + [\,\partial/\partial x\,(\mu\partial W/\partial x) + \partial/\partial y\,(\mu\partial W/\partial y) + \partial/\partial z\,(\mu\partial W/\partial z)\,]$$

where U V W are the velocity components in the x y z directions, P is pressure, ρ is the density of water and μ is its effective viscosity. The time averaging process introduces source like terms A B C into the momentum equations. Each is a complex function of velocity and viscosity gradients as indicated below:

$$A = \partial\mu/\partial y\ \partial V/\partial x - \partial\mu/\partial x\ \partial V/\partial y + \partial\mu/\partial z\ \partial W/\partial x - \partial\mu/\partial x\ \partial W/\partial z$$

$$B = \partial\mu/\partial x\ \partial U/\partial y - \partial\mu/\partial y\ \partial U/\partial x + \partial\mu/\partial z\ \partial W/\partial y - \partial\mu/\partial y\ \partial W/\partial z$$

$$C = \partial\mu/\partial y\ \partial V/\partial z - \partial\mu/\partial z\ \partial V/\partial y + \partial\mu/\partial x\ \partial U/\partial z - \partial\mu/\partial z\ \partial U/\partial x$$

Conservation of mass considerations give:

$$\partial P/\partial t + \rho\, c^2\,(\,\partial U/\partial x + \partial V/\partial y + \partial W/\partial z\,) = 0$$

Although water is basically incompressible, for mass conservation, FLOW 3D takes it to be compressible. Mass is used to adjust pressure at points in the grid when the divergence of the velocity vector is not zero.

A popular eddy viscosity model is known as the k-ε model where k is the local intensity of

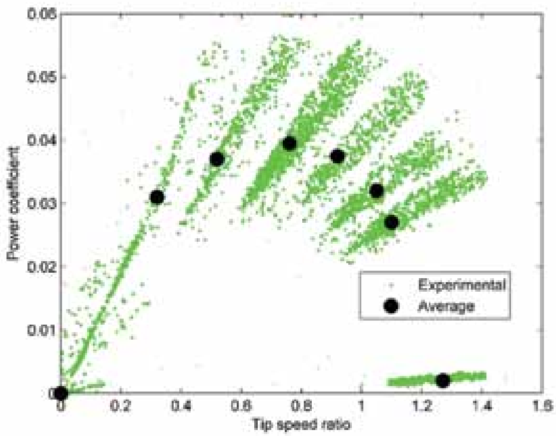

Figure 2: Data for the experimental Savonius rotor.

turbulence and ε is its local dissipation rate. Its governing equations are:

$$\partial k/\partial t + U\partial k/\partial x + V\partial k/\partial y + W\partial k/\partial z = T_P - T_D + [\,\partial/\partial x\,(\alpha\,\partial k/\partial x) + \partial/\partial y\,(\alpha\,\partial k/\partial y) + \partial/\partial z\,(\alpha\partial k/\partial z)\,]$$

$$\partial\varepsilon/\partial t + U\partial\varepsilon/\partial x + V\partial\varepsilon/\partial y + W\partial\varepsilon/\partial z = D_P - D_D + [\,\partial/\partial x\,(\beta\partial\varepsilon/\partial x) + \partial/\partial y\,(\beta\partial\varepsilon/\partial y) + \partial/\partial z\,(\beta\partial\varepsilon/\partial z)\,]$$

where

$$T_P = G\,\mu_t / \rho \qquad D_P = T_P\,C_1\,\varepsilon / k$$
$$T_D = C_D\,\varepsilon \qquad D_D = C_2\,\varepsilon^2 / k$$
$$\mu_t = C_3\,k^2 / \varepsilon \qquad \mu = \mu_t + \mu_l$$
$$\alpha = \mu/a \qquad \beta = \mu/b$$

where

$$G = 2\,[\,(\partial U/\partial x)^2 + (\partial V/\partial y)^2 + (\partial W/\partial z)^2\,] + [\,\partial U/\partial y + \partial V/\partial x\,]^2 + [\,\partial U/\partial z + \partial W/\partial x\,]^2 + [\,\partial W/\partial y + \partial V/\partial z\,]^2$$

where C_D, C_1, C_2, C_3, a and b are constants based on data from geometrically simple experiments, μ_l is the laminar viscosity, μ_t is extra viscosity due to eddy motion and G is a production function. The k-ε equations account for the convection, diffusion, production and dissipation of turbulence.

A new feature of FLOW 3D known as the General Moving Object (GMO) allows bodies to move through the grid. No other CFD package has this feature. The motions of the bodies can be prescribed or they can be coupled to the motion of the fluid. It allows for extremely complicated motions and flows. One can think of a GMO as a bubble in a flow where the pressure on the inside surface of the bubble is adjusted in such a way that its boundary matches the shape of a body. FLOW 3D uses a complex interpolation scheme to fit the body into the Cartesian grid.

For CFD, each governing equation is put into the form:

$$\partial M/\partial t = N$$

At points within the CFD grid, each governing equation is integrated numerically across a time step to get:

$$M(t+\Delta t) = M(t) + \Delta t\, N(t)$$

where the various derivatives in N are discretized using finite difference approximations. The discretization gives algebraic equations for the scalars P k ε at points where grid lines cross and algebraic equations for the velocity components U V W at staggered positions between the grid points. Central differences are used to discretize the viscous terms in the momentum and turbulence equations. To ensure numerical stability, a mix of central and upwind differences is used for the convective terms. Collocation or lumping is used for source terms. To march the unknowns forward in time, the momentum equations are used to update U V W, the mass equation is used to update P and correct U V W and the turbulence equations are used to update k and ε. The Semi Implicit Method for Pressure Linked Equations (SIMPLE) procedure is used to get pressure through an iterative process involving mass and momentum. Special wall functions are used to skip over the sharp normal gradients in velocity and turbulence near walls. With these functions, boundary conditions are applied just outside the boundary layer next to the wall and not at the wall itself.

For the simulation, the rotor was first drawn in SolidWorks. The geometry file was imported into FLOW 3D as an STL file. The thickness of the buckets of the rotor was made six times actual so that the grid employed could discretize them. The density of the rotor was adjusted to keep the total inertia of the rotor equal to the original prototype.

Figure 3 shows a typical grid used to model the rotor. It used three cell blocks. Each cell block can have its own cell size. However, here each had a cell size of 5 mm. The mesh in the figure is 10 times coarser than this. We tried finer mesh sizes and they gave basically the same results. We found it was very important to position the rotor well away from flow boundaries. The rotor was modelled as a GMO with freedom to rotate around the vertical axis.

The boundary conditions used for the simulation are shown in Figure 4. Fluid enters across the surface labelled V and leaves at the surfaces labelled O. The label G indicates grid overlap from one block of cells to the next. Non porous thin plate baffles, not shown in the figure, were used to model the top and bottom plates of the box used in the test setup.

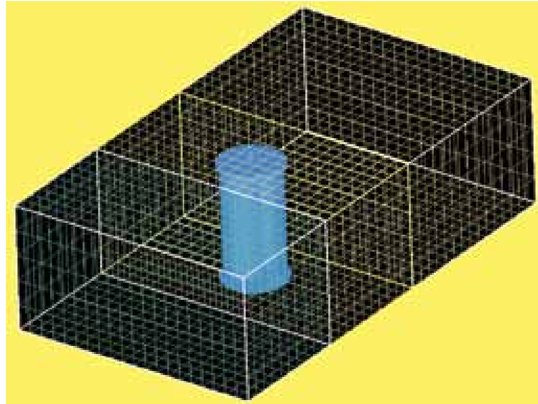

Figure 3: Computational mesh for the Savonius rotor.

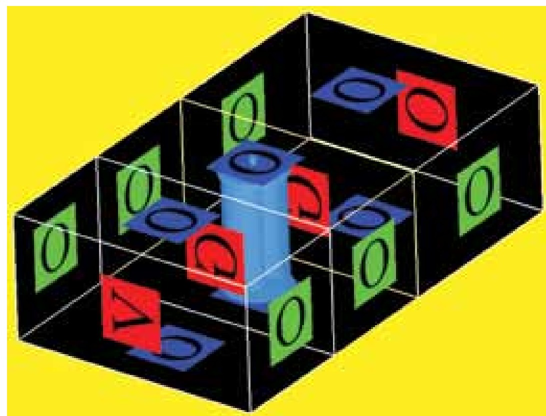

Figure 4: Boundary conditions for the Savonius rotor.

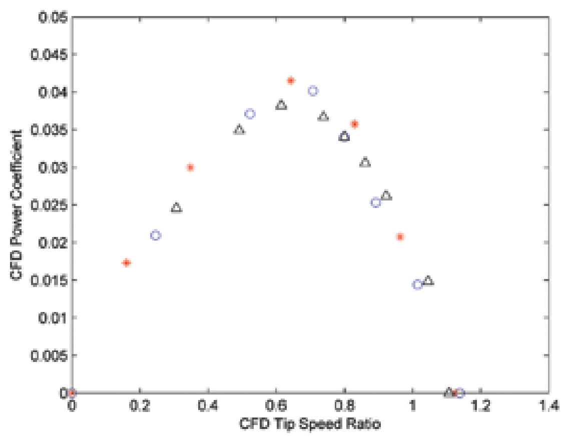

Figure 5: CFD power coefficient vs. tip speed ratio.
* Small o Medium Δ Large

COMPUTATIONAL RESULTS

The simulation was set up for 30 seconds duration to allow the rotor to reach a steady rotation cycle free of startup transients. In order to calculate the rotor power, the angular speed

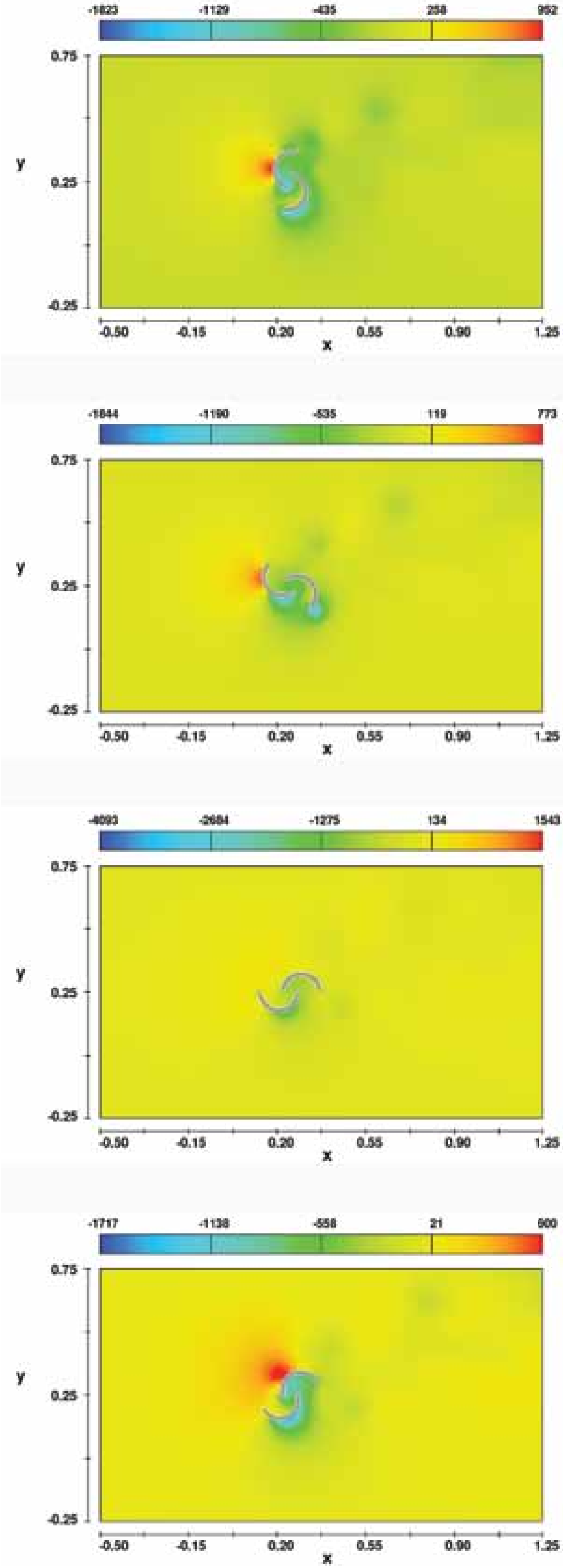

Figure 6: Pressure at steps in time.

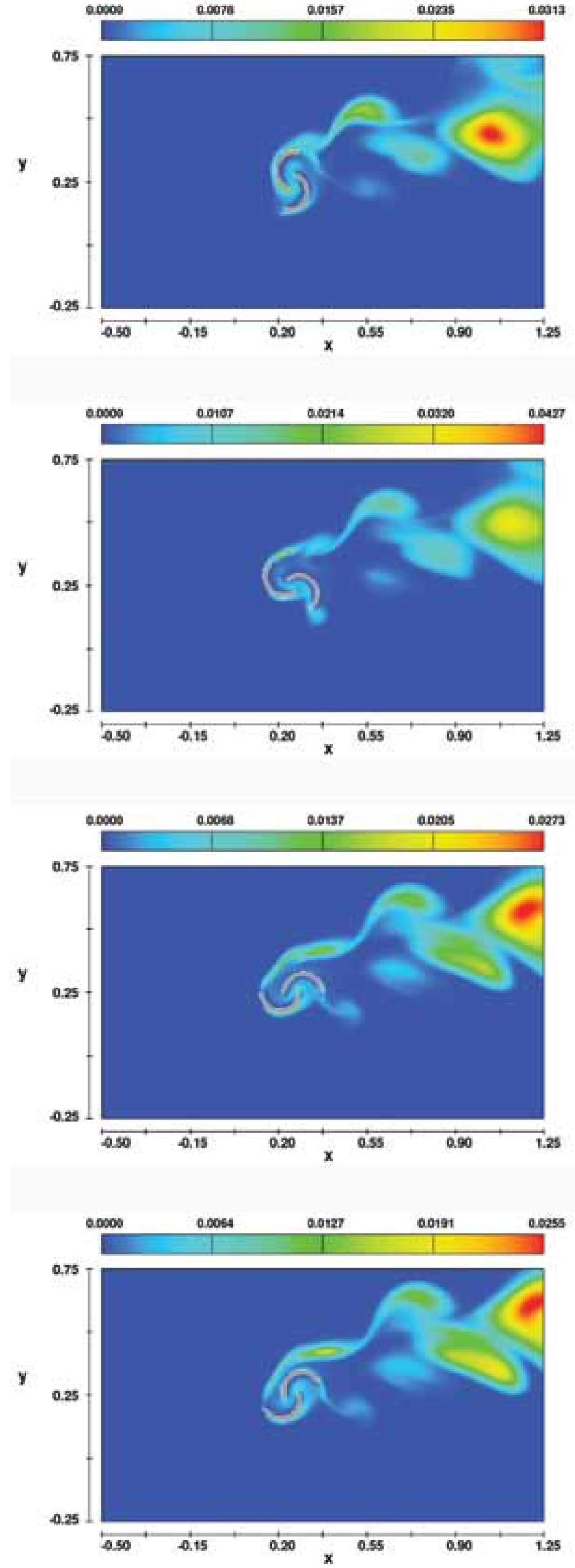

Figure 7: Turbulent energy at steps in time.

of the rotor was set and the torque on the rotor was recorded. Because of the geometry of the rotor, there are dead zones where torque is very low. The average torque times speed gave the rotor power. Three rotor sizes were tested. They had profile areas of 0.48 m^2, 0.088 m^2 and 0.066 m^2. These were the sizes tested in the experiment. The CFD power curves of the rotors are shown in Figure 5. As can be seen, the no load tip speed, the peak power coefficient and the peak tip speed are approximately the same for each rotor. In addition, the CFD results agree closely with test results.

The CFD simulation also gives details about the flow around the rotor. This can be for 2D slices through the rotor or for the full 3D rotor. Figure 6 shows the pressure around a 2D slice during a free wheel or no load case. High pressure is indicated in red and low pressure is indicated in blue. Note the stagnation pressure zones on the buckets of the rotor. Figure 7 shows the turbulent energy around the rotor for the free wheel case. One can see very turbulent zones downstream of the bucket moving into the stream. The simulation has subroutines that would allow one to study various control strategies for the rotor. In some preliminary work with this feature, the rotor became less prone to stalling in the dead zones when the control torque was set to zero in these zones.

CONCLUSION

This paper has shown that CFD can be used to study the behaviour of water current turbines. The behaviour of the CFD rotor was roughly the same as that of the experimental rotor. The CFD results confirm the scaling laws for turbines. Data from three different size rotors were found to fall close to the same power coefficient versus tip speed ratio curve. Our goal now is to use CFD to fine tune rotor geometry and study the performance of various rotor control strategies.

ACKNOWLEDGEMENTS

The authors wish to thank the Atlantic Innovation Fund and Memorial University of Newfoundland for their financial support. We also wish to thank Dr. Iqbal and Dr. Masek for their support.

REFERENCES

Flow Science [n.d.]. *Flow Science Inc*. Retrieved from www.flow3d.com.

Khan, N., Hinchey, M., Iqbal, T., and Masek, V. [2009]. *Performance of the Savonius rotor as water current turbine*. Journal of Ocean Technology, Vol. 2, No. 2, pp. 71-83.

Khan, N., Hinchey, M., Iqbal, T., and Masek, V. [2010]. *On scaling laws for Savonius water current turbines*. Journal of Ocean Technology, Vol. 5, No. 2, pp. 92-101.

Savonius, S.J. [1931]. *The Savonius S-rotor and its applications*. American Society of Mechanical Engineering, Vol. 53, No. 5.

Errata

In research previously conducted by the authors, the results of which were published in the JOT (Vol.4, No.2; Vol.5, No.2), for the derivation of the Betz limit, both $\mathbf{R}$ and R were incorrectly depicted by the same symbol. $\mathbf{R}$ indicates a power ratio while R indicates a speed ratio. Further, the authors indicate that the tip speed ratio for the rotor was not calculated properly. It is calculated properly in this paper. The following gives the correct derivation of the Betz limit.

Dividing P by the upstream power gives the power ratio

$\mathbf{R} = P / [\rho(V^2/2)VA]$

Letting R = W/V allows one to rewrite $\mathbf{R}$ as

$\mathbf{R} = (1-R^2)(1+R)/2$

Setting $d\mathbf{R}/dR$ equal to zero shows that a peak power ratio occurs when R is 1/3. Back substitution shows that the peak power ratio is $\mathbf{R}$=0.59. This is the Betz limit.